JOURNAL OF MATERIALS SCIENCE 19 (1984) 965–973

Carbides in iron-rich Fe–Mn–Cr–Mo–Al–Si–C systems

F. D. LEMKEY
United Technologies Research Center, East Hartford, CT 06108, USA
H. GUPTA, H. NOWOTNY, S. F. WAYNE
University of Connecticut, Storrs, CT 06268, USA

Duplex microstructures of iron-base superalloys, consisting of an austenitic matrix and a M_7C_3 carbide, can be produced within the Fe–Mn–Cr–Mo–Al (Si)–C systems. The stability regions of the carbides were inspected by means of isothermal sections of alloys in the quinary combination Fe–Mn–Cr–Mo–C for 70 at % metal and 30 at % carbon. For 35 at % iron the competing carbides are found to be M_2C, M_3C and the molybdenum cementite ($MoFe_2C$) in the arc-melted state, with $M_{23}C_6$ in the annealed state. In the quaternary system, Fe–Mn–Mo–C, a M_2C carbide forms, presumaby derived from a solid solution carbide, $(Mn, Mo)_2C$. In extracted carbides of cast alloys containing Fe–Mn–Cr–Mo–Al (Si)–C a considerable amount of the π-phase carbide occurs.

1. Introduction

It has been demonstrated that alloys containing 10 to 20 wt % manganese, 10 to 20 wt % chromium, up to 3 wt % carbon, with the balance iron can be produced with duplex microstructures, consisting of an austenitic matrix reinforced by aligned M_7C_3 carbide fibres [1]. Additions of molybdenum, aluminium and silicon have been envisaged to improve strength and oxidation resistance at high temperatures. A major task in the development of such ferrous superalloys is the characterization of the stability regions of the γ and the M_7C_3 phases. Few of the many investigations of eutectic (*in situ*) composites have examined the potential of aligned structures in iron-base superalloys. However, *in situ* composites, based on the Fe–Co–Cr–C quaternary system, were studied by van de Boomgaard *et al.* [2] who described alloys consisting of a metal matrix and the M_7C_3 carbide. They reported a drop in strength at 900° C, after an anneal at 950° C, due to the transformation of the M_7C_3 carbide into the $M_{23}C_6$ carbide.

Only a few investigations on multicomponent systems have been carried out and this is also true for ferrous alloys despite their technological importance. Detailed data such as phase analysis, region of solubility lattice parameters and morphology are available for equilibria of some ternaries. In particular the Fe–Cr–C system was subject of early studies, from which the high stability of the $(Cr, Fe)_7C_3$ carbide was derived. A more recent work [3] pertinent to the problem of ferrous superalloys deals with Cr–Mo steels equilibria, describing the M_7C_3 carbide as $(Cr, Fe, Mo)_7C_3$.

2. Carbides in the iron-base quinary system: Fe–Mn–Cr–Mo–C

Quantitative structural data on the M_7C_3 carbide have been reported by Dyson and Andrews for low carbon Cr–Mo steels after solution treatment and anneal [3]. These authors observed the M_7C_3 carbide with M = Cr, Fe, Mn and Mo in decreasing amounts with a typical formula, $(Cr_{4.9}Fe_{2.0}Mn_{0.2}Mo_{0.1})C_3$, which is close to M_7C_3 [3]. As the molybdenum content in the M_7C_3 appears to be small, the lattice parameters should increase with an increasing ratio of Cr/(Cr + Fe + Mn + Mo). Thus, the major change of the hexagonal unit cell is due to the partial substitution of chromium by iron in the stable carbide Cr_7C_3. From various investigations of the Fe–Cr–C ternary system [4] (up to 1 wt % carbon and

0022–2461/84 $03.00 + .12

from 0 to 29 wt% chromium), the only carbides present were shown to be $M_{23}C_6$, M_3C and M_7C_3; the first is in equilibrium with both α and γ, whereas M_3C and M_7C_3 are only in equilibrium with γ. There is little doubt that these carbides are stoichiometric, although in the case of the corresponding Fe–Mn–C system, a small deviation for the cementite phase $(Fe, Mn)_3C$ has been found [5]. The M_7C_3 to $M_{23}C_6$ transformation was also the subject of a detailed investigation by Beech *et al.* [6]. Similarly, the transformation of M_3C (cementite) to M_7C_3 in high-carbon chromium steel was studied and an *in situ* mechanism leading to internal faults of the M_7C_3 carbide, has been suggested [7]. With carbon present to 3 wt% and, in particular, molybdenum increasing to 10 wt%, the M_6C carbide (η-carbide) becomes predominant, as was recently shown by Krainer *et al.* [8]. according to an investigation in the Fe–Cr–Mo–C quaternary system (Mn-free), the occurrence of the carbides M_6C, $M_{23}C_6$, M_3C, M_7C_3 and the molybdenum cementite $MoFe_2C$ has been reported [9]. Two four-phase spaces ($\gamma + M_6C + M_3C + M_7C_3$) and ($\gamma + M_6C + M_{23}C_6 + M_7C_3$) were established in the region up to 12 wt% Cr, 14 wt% Mo and 2.5 wt% C for the non-variant equilibrium state at 1100° C. These authors express the opinion that the molybdenum cementite, also called ξ carbide, appears to have a composition closer to the η-carbides. Specifically for the M_7C_3 carbide, solubilities in the region of 22 to 43 wt% Cr, 13 wt% Mo were found in $(Fe, Cr, Mo)_7C_3$.

As continuing investigations are centred on generating and stabilizing duplex microstructures ($\gamma + M_7C_3$) under varying thermal conditions for ferrous alloys and in particular *in situ* composites, a detailed study of the metal–metal substitution in M_7C_3 and the competing carbides within the relevant systems was undertaken. While the congruently melting Cr_7C_3 is a stable phase, the analogous Fe_7C_3 exists as a metastable phase [10]. In terms of stability, the corresponding carbide Mn_7C_3 is intermediate. With regard to the crystal structure of these three M_7C_3 carbides and subsequently their formation of solid solutions, a clarification of differing assessments was presented only recently [11]. Although structurally closely related, three different types of unit cells, having trigonal, orthorhombic or hexagonal symmetry, have been reported. It was assumed that the various cells previously proposed are superlattices of a hypothetical disordered array. The orthorhombic symmetry, even in the case of Cr_7C_3 with a ratio b/a precisely $\sqrt{3}$, appears to be masked by twinning with an angle of 120°. It was shown that planar faults (antiphase boundaries) or twins (fault planes $\{10\bar{1}0\}$) occur and microdomains are formed [12]. Stacking faults in Cr_7C_3 were observed in electron diffraction patterns even earlier [6]. Similar behaviour appears to exist for M_7C_3 solid solutions of extracted carbides from white cast iron and chromium steels with M = Cr, Fe, V which derive from the Cr_7C_3-type structure [13], confirming Westgren's work [14]. The existence of a uniform $(Cr,Mn,Fe)_7C_3$ carbide assigned to this trigonal symmetry was proven for a considerable number of alloys [1].

3. Experimental details

Due to the importance of the M_7C_3 carbide in achieving strength at elevated temperatures, a set of alloys corresponding to a nominal composition M_7C_3 (M = Fe,Mn,Cr,Mo) were prepared and inspected by X-ray diffraction (Debye–Scherrer camera, diameter 57.3 mm) and optical microscopy techniques. The amount of iron was kept constant at 25 and 50 at % of the amount of transition elements. Some samples were prepared and characterized with 10 at % iron referred to the metal amount. The starting materials were: iron powder 99.9$^+$, manganese powder 99$^+$, chromium powder 99.95, molybdenum powder 99.9$^+$, carbon, graphite powder 99.5$^+$, all obtained commercially from Alfa Ventron. Pellets of approximately 1 g of powder mixtures, wrapped in tantalum foil, were encapsulated in evacuated quartz ampoules and sintered at 1100° C for 48 h. Half of each speciment was arc melted, followed by consecutive heat treatments at 1000° C for 48 h and at 700° C for 170 h. During arc melting a slight loss of manganese and carbon may occur, while no significant change in composition occurs for the sintered and furnace-cooled material. As the carbides (M_2C, M_7C_3, M_3C, $M_{23}C_6$ and M_6C) do not exhibit strong deviations from stoichiometry, one can expect the remaining phase to be either iron solid solutions (α or γ) or graphite. The only varying ratio of carbon to metal is within the γ (austenite). Furthermore, alloys were prepared by vacuum induction melting of foundry grade iron, ferromanganese, chromium, molybdenum, aluminium, silicon and carbon elements and cast [1]. From these cast alloys the carbides were extracted by means of a heated 10% alcoholic bromine solution.

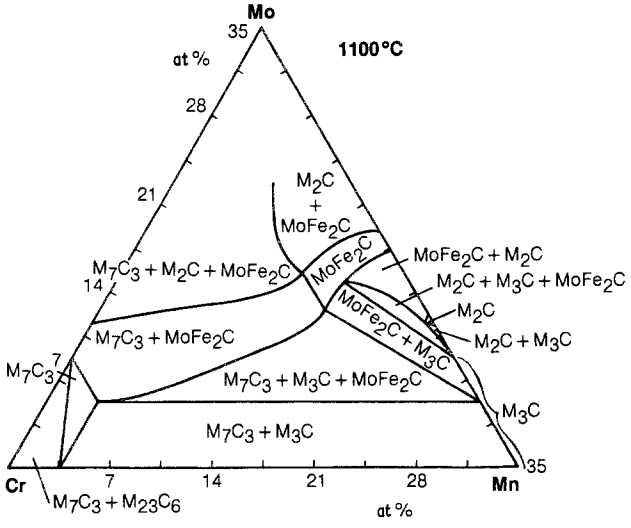

Figure 1 Fe–Mn–Cr–Mo–C (35 at % Fe and 30 at % C) equilibria at 1100° C.

4. Results and Discussion

The phase separation of the carbides for the sintered states of the quinary system, Fe–Mn–Cr–Mo–C, is presented in Fig. 1, which can be described as isothermal, (isobaric), at 35 at % iron and 30 at % carbon. There was no hint of the occurrence of intermetallics, but the molybdenum-rich portion was not explored. Furthermore the metal phase (α or γ) and graphite (or carbon-rich carbides) are not indicated in Fig. 1. Carbon-rich phases such as Cr_3C_2 or MC phases have not been detected. The wide occurrence of the M_7C_3 carbide in the presence of iron (35 at %). That means a narrow single phase region exists in the quinary system. In the region low in molybdenum (less than 7 at %), the M_3C carbide competes with the M_7C_3 carbide. The phase field with both these carbides is large, thus leaving the carbide M_7C_3 field relatively narrow. It should be noted that in the presence of 35 at % iron and 3.5 at % manganese the M_7C_3 carbide dissolves up to 5 at % molybdenum (carbide), but the solubility of the molybdenum carbide in the M_7C_3 carbide decreases as the amount of manganese increases at the expense of chromium. The lattice parameters of the M_7C_3 carbide are significantly lower than those of pure Cr_7C_3. An alloy of nominal composition $(Fe_{0.5}Mn_{0.05}Cr_{0.4}Mo_{0.05})_7C_3$, which is single phase, has cell parameters: $a = 1.395_3$ and $c = 0.4502$ nm. It indicates the substitution of the chromoum atom by the smaller sized iron and manganese atoms. Gradually increasing the amount of manganese at the expense of chromium does, however, yield a somewhat irregular decrease of the unit cell which might be due to the variety of space groups and formation of microdomains, especially at the iron-rich side of the M_7C_3 carbide [12]. In fact, for the set of sintered alloys of nominal composition $(Fe_{0.25}, Mn, Cr, Mo_{0.05})_7C_3$, the cell volume against concentration is a smoothly decreasing curve due to the substitution Cr/Mn in the M_7C_3 carbide (Fig. 2).

Most of the acr-melted (and quenched conditions) samples of nominal compositions 35 at % iron, 30 at % carbon with varying amounts of manganese and chromium were not in an equilibrium state. Thus, the analysis did not allow the establishment of a consistent phase distribution. Nonetheless, as is shown in Table I, the arc-melted alloys consist, except for the molybdenum-cementite, of those carbides which also occur in

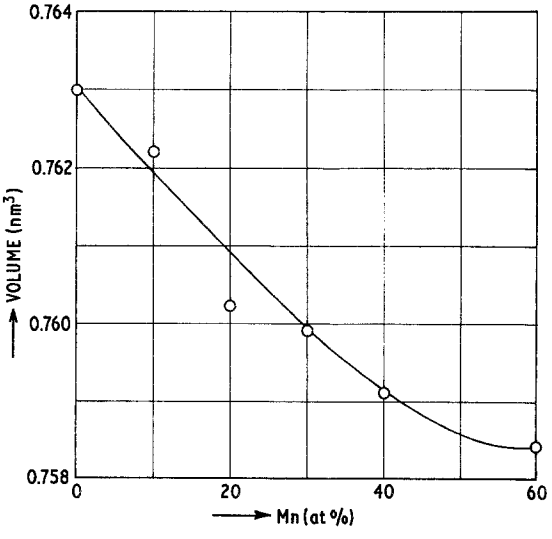

Figure 2 M_7C_3 cell volume against manganese concentration.

TABLE I Phase analysis of selected arc-melted alloys with nominal compositions $(Fe_{0.5}, Mn, Cr, Mo)_7C_3$

Atomic metal ratio				Phases present
Fe	Mn	Cr	Mo	
50	–	20	30	$Fe + M_2C$
50	10	10	30	$M_2C + M_7C_3 + Fe$
50	15	05	30	$M_2C + M_7C_3 + Fe$
50	20	–	30	$M_2C + Fe$
50	–	25	25	$M_2C + Fe$
50	05	20	25	$M_2C + Fe$
50	10	15	25	$M_2C + M_7C_3 + Fe$
50	20	05	25	$M_2C + Fe$
50	–	30	20	$M_2C + Fe + M_7C_3$
50	10	20	20	$M_2C + Fe + M_7C_3$
50	20	10	20	$M_7C_3 + M_2C + Fe$
50	30	–	20	$M_2C + Fe + MoFe_2C$
50	–	35	15	$M_7C_3 + Fe + M_2C$
50	05	30	15	$Fe + M_2C + M_7C_3$
50	15	20	15	$Fe + M_2C + M_7C_3$
50	25	10	15	$Fe + M_7C_3 + M_2C$
50	35	–	15	$Fe + M_2C + M_7C_3$
50	–	40	10	$Fe + M_7C_3 + M_2C$
50	10	30	10	M_7C_3
50	20	20	10	$M_7C_3 + M_2C + Fe$
50	25	15	10	$M_7C_3 + M_2C + Fe$
50	30	10	10	$M_7C_3 + M_3C + Fe$
50	40	–	10	$M_7C_3 + M_3C$
50	–	45	05	$M_7C_3 + Fe$
50	10	35	05	$M_7C_3 + Fe$
50	20	25	05	$M_7C_3 + Fe$
50	30	15	05	$M_7C_3 + Fe + M_3C$
50	35	10	05	$M_7C_3 + M_3C + Fe$
50	40	05	05	$M_7C_3 + M_3C$

TABLE II The occurrence of phase(s) in some of the selected arc-melted alloys with nominal compositions $(Fe \cdot 25\ Mn,Cr,Mo)_7C_3$ and $(Fe \cdot 1\ Mn,Cr,Mo \cdot 1)_7C_3$

Atomic metal ratio				Carbide(s) present
Fe	Mn	Cr	Mo	
25	10	55	10	7/3 carbide
25	30	35	10	7/3 carbide
25	35	30	10	7/3 carbide
25	45	20	10	7/3 carbide
25	65	–	10	$(Mo,Mn)_2C + Fe$
25	–	70	05	7/3 carbide
25	10	60	05	7/3 carbide
25	30	40	05	7/3 carbide
25	50	20	05	7/3 + 3/1 carbides
25	60	10	05	7/3 + 3/1 carbides
25	70	–	05	7/3 + 3/1 carbides
10	–	80	10	7/3 + 23/6 carbides
10	30	50	10	7/3 carbide
10	50	30	10	7/3 carbide
10	80	–	10	$(Mo,Mn)_2C + Fe$

The atomic metal ratio 10 and 25 for iron corresponds to 7 and 17.5 wt% Fe respectively

the sintered state. The molybdenum-cementite obviously disappears after melting. Fewer samples exhibit the occurrence of the M_7C_3 carbide as compared to the sintered state; however, M_2C shows up much more frequently. Iron also separates out from most of these alloys in the form of solid solutions. The corresponding arc-melted alloys have a higher amount of manganese chromium and molybdenum in the M_7C_3 carbide and subsequently a larger unit cell.

Arc-melted alloys, 7 and 17.5 at% iron and 30 at% carbon consist mainly of M_7C_3 carbide, as is shown in Table II. Some of these alloys which have higher concentration of manganese were is found to contain a subcarbide, M_2C.

4.1. The subcarbide M_2C

Because of the high thermochemical stability of Mo_2C, this carbide frequently occurs in molybdenum-containing steels. With respect to the solubility of Mo_2C for iron (carbide), there is disagreement. For a formula $(Fe_{0.05}Mo_{0.95})C$, Surovoi *et al.* [15] have reported cell parameters: $a = 0.3000$, $c = 0.4719$ nm, where the c-axis is significantly smaller than for pure Mo_2C. In a phase diagram Fe–Mo–C, calculated for 1000° C by Uhrenius and Harwig [16], a small Mo/Fe substitution in Mo_2C has been taken into account, but a recent compilation by Holleck [17] does not reveal any solubility. It also was found that the change in lattice parameters was scarcely detectable, but a Mo_2C sample having 2 at% iron was homogeneous [18]. One can assume that the decrease in cell parameters may be compensated by more carbon in the interstices. On the other hand, manganese and chromium (carbides) dissolve considerably in Mo_2C, up to 15 mol% (800° C) and 70 mol% (1350° C) respectively referring to Mn_7C_3 [19] and Cr_7C_3 [20]. Investigating carbides in a M-50 tool steel, Bridge *et al.* [21] derived for the M_2C carbide a formula: $(Mo_{0.71}Fe_{0.14}Cr_{0.15})_2C$, based on the assumption that the subcarbide only involves these metals.

In extracted products [22] of chromium-free alloys of composition 10 wt% Mn; 10 or 4 wt% Mo; 1 wt% C; 2 wt% Al, balance iron, the M_2C carbide occurs as a major constituent. First based on a hexagonal cell, the parameters were found to be: $a = 0.2984_5$ and $c = 0.4704_8$ nm, significantly smaller than those for pure Mo_2C. An EXAX analysis of this extracted carbide (85 at% Mo, 9.3 at% Fe and 5.0 at% Mn of the total amount

of metals) clearly indicates substitution of molybdenum by iron and manganese in the subcarbide, ignoring the fact that some γ was present.

Parthé *et al.* [23] have shown that Mo_2C is pseudohexagonal (space group *P*bcn and Rudy *et al.* [24] found one hexagonal and one orthorhombically distorted molybdenum subcarbide, the stability of these depending on temperature and carbon concentration. The powder pattern of the extracted carbide $(Mo, Fe, Mn)_2C$ was shown to crystallize in the orthorhombic distorted cell with: $a = 0.4708$, $b = 0.5931$ and $c = 0.5159$ nm (see Table III). Note that a corresponds to c_{hex}, b to $2a_{hex}$, and c to $a\sqrt{3}$. The decrease of the cell parameters of $(Mo, Fe, Mn)_2C$ as compared to Mo_2C is obvious.

An interesting finding of the present work involves the manganese-rich portion of the section at 30 at% carbon of the Fe–Mn–Cr–Mo–C system. In the binary Mn–C, a high temperature phase, called ϵ-Mn_4C_{1+x} having a hexagonal close packed metal array has been reported [25]. This carbide, difficult to corroborate [26, 27], was obviously found to occur with the cell parameters: $a = 0.2709$, $c = 0.4423$ nm. In the present study there were several arc-melted alloys observed, consisting of a subcarbide with a close packed metal array besides α-iron solid solutions. The intitial atomic metal ratio was, for example, Fe(1) Mn(8) Mo(1). Thus the existence of a subcarbide (Mn, $Mo)_2C$ is most likely. As can be seen from Table IV, the evaluation of the powder pattern of such an alloy (Fe–Mn–Mo–C) fits perfectly with a hexagonal subcarbide having the cell parameters: $a = 0.2778$ and $c = 0.450_0$ nm. These values agree rather well with a formula $Mn_{1.5}Mo_{0.5}C$ on the assumption of a linear increase from a "Mn_2C" carbide to Mo_2C (Fig. 3). Interestingly, the higher carbon defect in ϵ-Mn_4C_{1+x} as compared to a subcarbide is consistent with almost ideal c/a ratio [25]. Most of the subcarbides exhibit a rather lower c/a ratio than ~ 1.63. In the case of (Mn, $Mo)_2C$ the ratio is close to this value but somewhat lower. From these findings one cannot exclude that the ϵ-Mn_4C_{1+x} carbide is a Mo-stabilized carbide. As the high temperature modification of Mo_2C is hexagonal, as are $Mn_{1.5}Mo_{0.5}C$ and ϵ-Mn_4C_{1+x}, continuous solid solutions may form at high temperatures. In fact, the (Mn, $Mo)_2C$ subcarbide vanishes in all alloys having an iron content of up to 17.5 at% after annealing at 1000° C for 50 h.

The arc-melted and quenched alloys with 7.0, 17.5 and 35 at% iron and 30 at% carbon were not fully in equilibrium after the above mentioned heat treatment. Besides the manganese-rich corner, the metal phase (iron solid solutions) is widely occurring. Most significantly, molybdenum-cementite, observed in the sintered state but not after arc melting, shows up again after annealing. It does not occur as frequently, however, as it did in the sintered condition.

TABLE III Powder data for extracted carbide of alloy 10 wt% Mn, 10 wt% Mo, 2 wt% Al, 1 wt% C, balance Fe; Cr$K\alpha^+$

Intensity	d_{obs} (nm)	d_{calc} (nm)	Index orthorh.	Index pseudohex.
w	0.2576	0.2579	(002)}	
		0.2570	(021)}	(10$\bar{1}$0)
w	0.2341	0.2354	(200)	(0002)
st	0.2520	0.26262	(102)}	
		0.2256	(121)}	(10$\bar{1}$1)
m	0.2120	0.2125		γ(111)
w	0.1949	0.1946	(022)	
m	0.1720	0.1739	(202)}	
		0.1739	(221)}	(10$\bar{1}$2)
m	0.1491	0.1487	(023)}	(11$\bar{2}$0)
w	0.1482	0.1482	(040)}	
m	0.1343	0.1341	(302)}	(10$\bar{1}$3)
m	0.1339	0.1339	(321)}	
m	0.1302	0.1301		γ(220)
m	0.1262	0.1259	(223)}	(11$\bar{2}$2)
w	0.1256	0.1254	(240)}	
m	0.1244	0.1247	(104)}	(20$\bar{2}$1)
w	0.1237	0.1241	(142)}	
m, d	0.1179	0.1178	(400)	(0004)

st = strong; m = medium; w = weak; d = diffuse.

TABLE IV Powder data of an arc-melted alloy of nominal composition Fe(0.1) mn(0.8) Mo(0.1) C(3/7); Cr$K\alpha$

Intensity	d_{obs} (nm)	d_{calc} (nm)	Index	Phase
m	0.2408	0.2406	(10$\bar{1}$0)	subcarbide
m	0.2250	0.2262	(0002)	subcarbide
st	0.2126	0.2125	(10$\bar{1}$1)	subcarbide
vw	0.2038	012023	(110)	α-Fe
w	0.1649	0.1646	(10$\bar{1}$2)	subcarbide
m	0.1393	0.1398	(11$\bar{2}$0)	subcarbide
m	0.1277	0.1278	(10$\bar{1}$3)	subcarbide
st, d	0.1186	0.1184	(11$\bar{2}$2)	subcarbide
st, d	0.1167	0.1168	(211)	α-Fe
		0.1163	(20$\bar{2}$1)	subcarbide

Subcarbide $(Mn, Mo)_2C$: $a = 0.2778$ nm, $c = 0.450_0$ nm.
α-Fe: $a \sim 0.286$ nm.
st = strong; m = medium; w = weak; vw = very weak; d = diffuse.

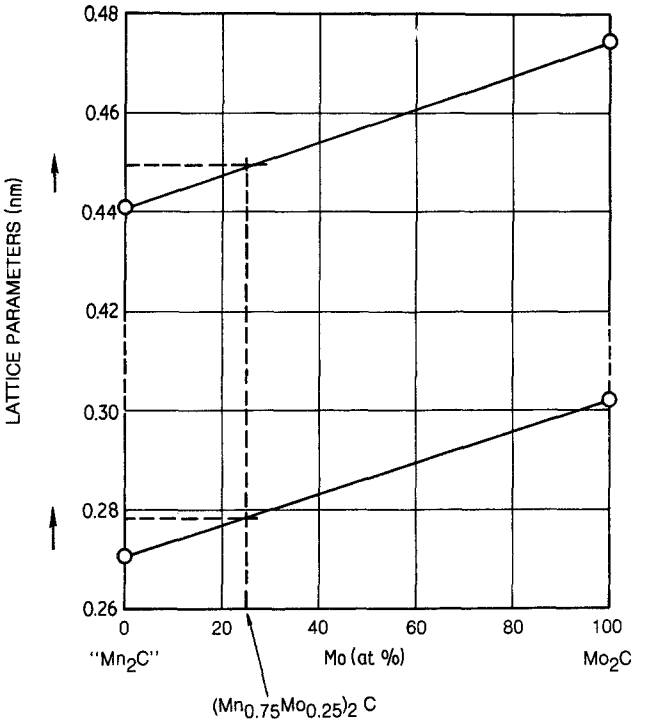

Figure 3 Mn_2C–Mo_2C lattice parameter dependence.

The phase distribution for the alloys after an additional anneal at 700° C for 170 h is presented in Fig. 4. It clearly indicates the disappearance of iron phase (iron-solid solutions). As mentioned earlier this iron solid solution appears after arc melting, not after sintering. As compared to the sintered state, the homogeneous region of the molybdenum cementite extends to about 10 mol% each of chromium carbide and manganese carbide for 35 at % iron and 30 at % carbon. On the other hand the cementite phase (M_3C) seems to dissolve up to 8 mol% molybdenum carbide and 6 mol% chromium carbide for 21 at % manganese, 35 at % carbon.

For alloys with 7.0 and 17.5 at % iron, 30 at % carbon, there is not much difference when compared to annealed conditions at 1000° C. The $M_{23}C_6$ carbide is present in a large number of samples, whereas M_2C is altogether absent. Lattice parameters of selected alloys for both annealing temperatures are listed in Table V. One should note that, as expected, no η-carbide (M_6C) occurs for the chosen concentration sections.

Optical micrographs confirm the findings of

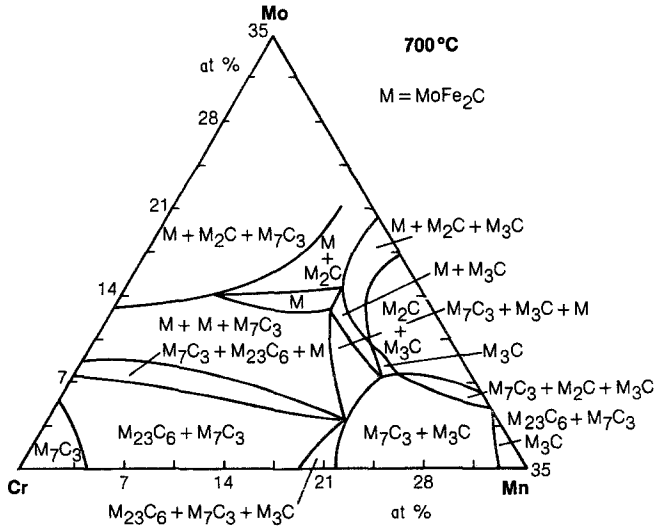

Figure 4 Fe–Mn–Cr–Mo–C (35 at % Fe and 30 at % C) equilibria at 700° C.

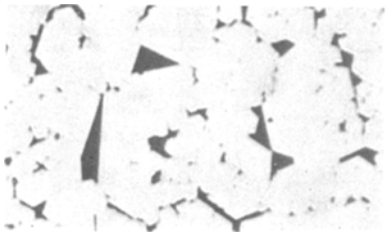

Figure 5 Arc-melted alloy Fe(17.5) Cr(49) Mo(3.5) C(30); almost all M_7C_3 carbide. 400X.

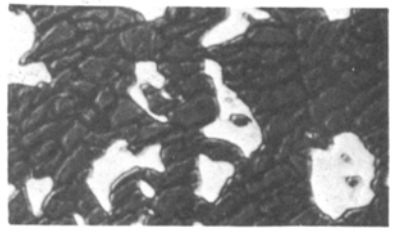

Figure 7 Annealed (1000° C) alloy Fe(35) Mn(28) Cr(3.5) Mo(3.5) C(30); $M_7C_3 + M_3C + M_2C$. 400X.

X-ray diffraction analysis. In Figs. 5 to 8 typical micrographs show the cell character and the hexagonal or pseudohexagonal symmetry of the M_7C_3 carbides for various compositions, in both arc melted and annealed states.

4.2. The π-phase (carbide) in iron base alloys Fe–Mn–Cr–Mo–Al–C

Extracted carbide products of a cast alloy 15 wt% Mn, 10 wt% Cr, 4 wt% Mo, 1.5 wt% C, 2 wt% Al, balance Fe, have been shown to consist of a phase having the β-Mn type metal array and a minor amount of $M_{23}C_6$ (Table VI). It should be mentioned that the matrix of the above cast alloy was almost all γ; only traces of α were present. There is a complete fit in indexing for the carbides, and the intensities compare perfectly to those for the β-Mn type metal array. Considering the relatively large lattice parameter ($a = 0.639_5$ nm), it is more likely that there is a carbide present than an intermetallic. This assumption is supported by the fact that manganese iron substitution is supposed to decrease the cell parameter. Furthermore the carbide is, in general, more stable against the extraction solution. Extraction of a cast alloy (Al-free), with 15% Mn, 5% Cr, 10% Mo, 1.5% C, balance Fe, yields a π-carbide having a cell parameter $a = 0.643$ nm. This cell parameter is much larger than that for β-Mn ($a = 0.632$ nm), but smaller than for the complex carbide Mo_3Al_2C ($a = 0.686_0$ nm), another filled up ordered β-Mn type structure [28].

Carbides [29] and nitrides [30] with filled up β-Mn parent lattice, called π-phases, have been observed earlier. These carbides form in Fe–Cr–W–C alloys after quenching from 1400° C but cannot be detected in the carbon-free systems Fe–Cr–W or Fe–Cr–Mo. Manganese itself favours the β-Mn structure, which tendency is further enhanced by iron and aluminium. This can be seen from the large domain of the β-Mn solid solutions in the ternary system Fe–Mn–Al [31]. Furthermore, molybdenum and aluminium form, in the presence of carbon, a filled up, ordered β-Mn structure [28] (see Table VI). From an EDAX analysis of this extracted carbide, it can clearly be seen that chromium, molybdenum and aluminium preferentially enter the π-carbide, while manganese distributes equally between the matrix and the carbide. The amount of iron in the π-carbide is roughly half of that in the matrix. The lattice parameter of the $M_{23}C_6$ carbide ($a \approx 1.062$ nm) indicates there is less iron and manganese incorporated. Nevertheless, the amount of $M_{23}C_6$ in the extracted carbide does not appear to change the distribution between π and γ significantly. A ratio of interstitial atom to metal atom of 1/5 indicates a complete filling of the octahedral voids in $4a$ of space groups $P4_132$; that means only a partial filling occurs according to the approximative formula

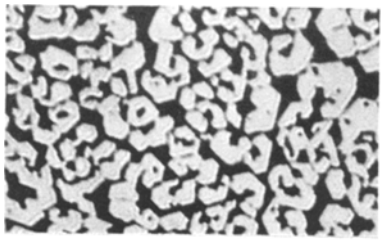

Figure 6 Arc-melted alloy Fe(17.5) Mn(42.0) Cr(7.0) Mo(3.5); mainly $M_7C_3 + M_3C$ carbides. 400X

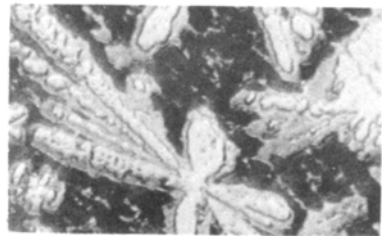

Figure 8 Annealed (700° C) alloy; Fe(35) Mn(17.5) Mo(17.5) C(30); $Mo_2C + MoFe_2C + M_3C$ carbides. 400X

TABLE V Lattice parameters of carbides in arc-melted and annealed alloys at 70 at.% metal and 30 at.% carbon

Atomic metal ratio				Annealing temperature (°C)	Lattice parameters (nm)		
Fe	Mn	Cr	Mo				
					M_3C		
					a	*b*	*c*
50	15	25	10	700	0.5051	0.6785	0.4592
25	60	10	05	1000	0.5106	0.6783	0.4558
					M_2C		
					a	*c*	
50	25	05	20	700	0.2978	0.4676	
50	30	05	15	1000	0.2975	0.469	
50	40	–	10	1000	0.2979	0.4698	
					M_7C_3		
					a	*c*	
50	10	30	10	700	1.3991	0.4505	
50	15	25	10	700	1.3999	0.4509	
25	50	20	05	1000	1.3954	0.4524	
25	60	10	05	1000	1.3915	0.4533	
					$M_{23}C_6$		
					a		
50	15	25	10	700	1.0551		
25	50	20	05	1000	1.0581		

$(Fe_{2.0}Mn_{0.7}Cr_{1.0}Mo_{0.4}Al_{0.9})C_x$ $(x \approx 1/3)$ for the aluminium-containing alloy.

Interestingly enough, silicon-containing arc-melted samples of nominal composition 10 wt% Mn, 20 wt% Cr, 1 wt% Mo, 7.5 wt% Si, 1.5 wt% C, balance Fe appeared to be an almost homogeneous alloy consisting of π-phase. A typical EDAX analysis was 13 wt% Mn, 26 wt% Cr, 1 wt% Mo, 12 wt% Si, 0.8 wt% C, balance Fe. The lattice parameter was found to be $a = 0.6213_5$ nm.

TABLE VI Powder data of extracted carbide, Cr$K\alpha$; alloy 15 wt% Mn, 10 wt% Cr, 4 wt% Mo, 2 wt% Al, 1.5 wt% C, balance Fe

Intensity	d_{obs} (nm)	d_{calc} (nm)	Phase	Index
vw$^+$	0.2378	0.2375	$M_{23}C_6$	(420)
vw	0.2162	0.2168	$M_{23}C_6$	(422)
st	0.2126	0.2131	π	(221)(300)
vw$^+$	0.2048	0.2044	$M_{23}C_6$	(333)(511)
m	0.2017	0.2022	π	(310)
w	0.1921	0.1928	π	(311)
vw	0.1877	0.1877	$M_{23}C_6$	(440)
vw	0.1790	0.1795	$M_{23}C_6$	(531)
vw	0.1712	0.1709	π	(321)
w	0.1506	0.1507	π	(330)(411)
w	0.1422	0.1430	π	(420)
vw	0.1278	0.1279	π	(430)(500)
st	0.1254	0.1254	π	(510)(431)
m	0.1229	0.1230	π	(333)(511)
st$^+$	0.1188	0.1187	π	(520)
m$^+$	0.1168	0.1167	π	(521)

st = strong; m = medium; w = weak; vw = very weak.

5. Conclusion

Optimizing the properties of high carbon iron-base superalloys with duplex microstructure $\gamma + M_7C_3$ carbide demands analysis within a seven-component system. Following the mode for establishing partial phase diagrams, data are provided for the quinary system: Fe–Mn–Cr–Mo–C at 30 at% carbon. From isothermal sections, the competing carbides are characterized according to a pseudo-ternary phase diagram at 35 wt% iron. The occurrence of the M_7C_3 carbide is favoured at the chromium corner, the M_3C carbide at the manganese corner, while M_2C carbide and the molybdenum cementite are predominant with increasing amounts of molybdenum. A Mn–Mo-carbide is also formed in extracted products of chromium-free cast alloys. Similarly, extractions of alloys containing Fe–Mn–Cr–Mo–Al(Si)–C have shown the presence of the π-carbide. Lattice parameters for the various carbides are reported.

Acknowledgement

The authors wish to acknowledge gratefully the support of NASA Lewis Research Center under the COSAM project, Grant MAG3-271.

References

1. F. D. LEMKEY, E. R. THOMPSON, J. C. SCHUSTER and H. HOWOTNY, in "In Situ Composites IV" Vol. 12 (Elsevier-North Holland, Boston 1982).
2. J. VAN DEN BOOMGAARD and L. R. WOLFF, *Philips Res. Repts.* **27**, (1972) 509; A. M. J. G. VAN RUN, Proceedings of the Conference on *In Situ* Composites, Lakeville, CT (1972).
3. D. J. DYSON and K. W. ANDREWS, *J. Iron Steel Inst.* **207** (1969) 208.
4. L. R. WOODYATT and G. KRAUSS, *Met. Trans. A.* **7A** (1976) 983.
5. L. BREWER, J. CHIPMAN and S. G. CHANG, in "Metals Handbook", 8th edn (American Society for Metals, 1961.
6. J. BEECH and D. H. WARRINGTON, *J. Iron Steel Inst.* **204**, (1966) 460.
7. A. INOUE, S. ARAKAWA and T. MASUMOTO, *Trans. Jpn. Inst. Metals* **19** (1978) 11.
8. E. KRAINER, *Berg-u.Hüttenm. Mh.* **127** (1982) 117.
9. E. STASKA, R. BLÖCH and A. KULMBURG, *Mikrochimica Acta* (Suppl. 5) (1974) 111.
10. H. C. ECKSTROM and W. A. ADCOCK, *J. Amer. Chem. Soc.* **72** (1950) 1042.
11. J. P. MORNIROLI and M. GANTOIS, paper presented at the VIIth International Conference on Transition Element Compounds, 21–25 June, 1982, Grenoble, France; to appear in *J. Appl. Crystallogr.*
12. E. BAUER-GROSS, J. P. MORNIROLI, G. LE CAER and C. FRANTZ, *Acta Metall.* **29** (1981) 1983.
13. W. DUDZINSKI, J. P. MORNIROLI and M. GANTOIS, *J. Mater. Sci.* **15** (1980) 1387.
14. A. WESTGREN, *Jernkont. Am.* **119** (1935) 231.
15. YU, N. SUROVOI, V. I. ALEXEEV and L. A. SCHWARZMAN, *Izv. Akad. Nauk SSSR, Neorg. Mater.* **1** (1965) 1816.
16. B. UHRENIUS and H. HARWIG, *Met. Sci.* **9** (1975) 67.
17. H. HOLLECK, Report KfK 3087B (1981) Karlsruhe, GFR.
18. J. C. SCHUSTER, unpublished.
19. V. S. TELEGUS, YU' B' KUZ'MA and M. A. MARKO, *Porosh, Met.* **11** (1971) 56.
20. YU. B. KUZ'MA and T. F. FEDEROV, *ibid.* **11** (1965) 62.
21. J. E. BRIDGE, Jr., G. N. MARINAR and T. V. PHILIP, *Met. Trans.* **2** (1971) 2209.
22. F. D. LEMKEY and H. NOWOTNY, unpublished.
23. E. PARTHÉ and V. SADAGOPAN, *Acta Crystallogr.* **16** (1963) 202.
24. E. RUDY, "Compendium of Phase Diagrams", Part V (1979).
25. R. BENZ, J. F. ELLIOT and J. CHIPMAN, *Met. Trans.* **4** (1973) 1449.
26. G. PAPESCH, Thesis, University of Vienna (1977).
27. J. C. SCHUSTER and H. NOWOTNY, *Z. Metallkde.* **72** (1981) 63.
28. W. JEITSCHKO, H. NOWOTNY and F. BENESOVSKY, *Mh. Chem.* **94** (1963) 247.
29. H. J. GOLDSCHMIDT, *Metallurgia* **56** (1957) 17.
30. D. A. EVANS and K. H. JACK, *Acta Crystallogr.* **10** (1957) 769.
31. D. J. SCHMATZ, *Trans. TMS, AIME* **215** (1959) 112.

Received 15 February
and accepted 21 July 1983